JARO 15: 707–719 (2014)
DOI: 10.1007/s10162-014-0476-6


JARO
Journal of the Association for Research in Otolaryngology

*Research Article*

# Systemic Lipopolysaccharide Compromises the Blood-Labyrinth Barrier and Increases Entry of Serum Fluorescein into the Perilymph

Keiko Hirose,[1] Jared J. Hartsock,[1] Shane Johnson,[2] Peter Santi,[2] and Alec N. Salt[1]

[1]*Department of Otolaryngology, Washington University School of Medicine, 660 South Euclid Avenue, Campus, Box 8115, St. Louis, MO 63110, USA*
[2]*Department of Otolaryngology, University of Minnesota, Minneapolis, MN, USA*

Received: 13 December 2013; Accepted: 3 June 2014; Online publication: 21 June 2014

## ABSTRACT

The blood vessels that supply the inner ear form a barrier between the blood and the inner ear fluids to control the exchange of solutes, protein, and water. This barrier, called the blood-labyrinth barrier (BLB) is analogous to the blood-brain barrier (BBB), which plays a critical role in limiting the entry of inflammatory and infectious agents into the central nervous system. We have developed an in vivo method to assess the functional integrity of the BLB by injecting sodium fluorescein into the systemic circulation of mice and measuring the amount of fluorescein that enters perilymph in live animals. In these experiments, perilymph was collected from control and experimental mice in sequential samples taken from the posterior semicircular canal approximately 30 min after systemic fluorescein administration. Perilymph fluorescein concentrations in control mice were compared with perilymph fluorescein concentrations after lipopolysaccharide (LPS) treatment (1 mg/kg IP daily for 2 days). The concentration of perilymphatic fluorescein, normalized to serum fluorescein, was significantly higher in LPS-treated mice compared to controls. In order to assess the contributions of perilymph and endolymph in our inner ear fluid samples, sodium ion concentration of the inner ear fluid was measured using ion-selective electrodes. The sampled fluid from the posterior semicircular canal demonstrated an average sodium concentration of 145 mM, consistent with perilymph. These experiments establish a novel technique to assess the functional integrity of the BLB using quantitative methods and to provide a comparison of the BLB to the BBB.

**Keywords:** LPS, cochlear fluid, blood-perilymph barrier, vascular permeability, inflammation

## INTRODUCTION

Blood vessels form a semipermeable barrier that permits the delivery of oxygen and controls the movement of cells, proteins, and ions from the blood into the peripheral organs. The vascular bed that perfuses the brain is highly specialized and limits the trafficking of molecules and cells into the central nervous system. Similar specialization has been observed in blood vessels that perfuse the inner ear. Maintaining a strictly controlled ionic and chemical environment in the inner ear requires that these barriers between the serum and inner ear fluids to be highly regulated. This barrier, referred to as the blood-labyrinth barrier (BLB), is thought to be essential for maintenance of normal hearing, because compromise would result in alterations of the ionic composition of inner ear fluids that could affect the endocochlear potential as well as other features of the inner ear environment. Loss of capillary integrity in other organs results in excessive fluid shifts, changes

*Correspondence to*: Keiko Hirose · Department of Otolaryngology · Washington University School of Medicine · 660 South Euclid Avenue, Campus, Box 8115, St. Louis, MO 63110, USA. Telephone: 314-454-4033; fax: 314-454-2174; email: keiko_hirose@post.harvard.edu

in electrolyte balance, and altered vascular permeability to proteins and cells. Such processes may occur in the inner ear in cases of local and systemic inflammation, but little is known about how changes in vascular permeability affect function.

Protein and amino acid levels differ considerably between perilymph, plasma and CSF although electrolyte composition is similar between the three fluids (Scheibe and Haupt 1985; Hara et al. 1989; Thalmann et al. 1992). Differences in chemical composition between perilymph and blood are made possible through the existence of the BLB (Fregni and Poli 1954; Juhn and Rybak 1981). Entry of $^{22}Na$ from serum into perilymph was found to occur more slowly than into CSF or into the fluids of the eye (Choo and Tabowitz 1964) where the amount of entry for different substances declined as the molecular weight of the substance increased (Juhn et al. 1982).

In the central nervous system, the blood-brain barrier (BBB) serves a similar purpose, and the cellular structures involved in the maintenance of the BBB are the subject of much study (Takeshita and Ransohoff 2012; Holman et al. 2011; Williams et al. 2001; Engelhardt and Ransohoff 2012; Wang et al. 2008). In the brain, the BBB is composed of endothelial cells, pericytes, and astrocyte end-feet that form the glia limitans and wall off the outer surfaces of blood vessels from the brain parenchyma. Within the glia limitans, between the endothelial cell and the astrocytes live the perivascular macrophages, which patrol this area. Pericytes, specialized cells that also occupy the perivascular space, are important in the development and maintenance of the blood-brain barrier. The density of pericytes outside the endothelial walls in part determines the relative permeability of the BBB (Daneman et al. 2010). In the inner ear, the cells that create the BLB are less clear, but they include the endothelial cells, pericytes, and likely other specialized cells that are not yet identified. It is possible that cochlear macrophages serve a role similar to perivascular macrophages in the brain, but the functional role of perivascular macrophages has not been clearly demonstrated. The blood vessels that travel through perilymph-filled spaces such as the spiral ligament, spiral limbus, modiolus, and osseous spiral lamina all contribute to the blood-labyrinth barrier to insulate the perilymph from the contents of blood vessels and are assessed by our technique described here of perilymph sampling. The strial vessels contain other specialized barriers that are not assessed in these experiments due to the tight junctions that separate the intrastrial fluid from the perilymph.

Traditional studies in the central nervous system have employed methods such as dye exclusion tests, radioactive tracers, as well as in vitro models to assess the integrity of the BLB and the BBB (Rossner and Tempel 1966; Wispelwey et al. 1988; Zhang et al. 2013). Agents such as Evans blue dye or fluorescein-tagged molecules can be effective to determine sites of vascular leakage where there are large volumes of tissue that are sparsely vascularized (Nishioku et al. 2009; Fernandez-Lopez et al. 2012; He et al. 2014). However, the inner ear of the mouse is tiny, the vessels are in close proximity to the tissues and fluids of interest, and sectioning the inner ear and imaging those sections to determine the extent of dye extravasation from vessels into adjacent tissues can pose challenges of interpretation. Sectioning of tissue can result in transfer of dye outside of vessels, particularly if the vessels are dense and the extravascular tissue is sparse. Finally, providing an objective, quantitative assessment of vascular leakage can be complicated when using imaging techniques (Kastenbauer et al. 2001). In these experiments, we provide a quantitative and objective method to assess BLB permeability by injecting sodium-fluorescein intravenously, and measuring the content of fluorescein in the perilymph and in the serum of live, anesthetized mice to determine what percentage of the serum levels of fluorescein enters the inner ear. We find that LPS consistently compromises the BLB and the BBB and that fluorescein entry into the inner ear is facilitated by systemic inflammation induced by LPS.

## MATERIALS AND METHODS

### Animals

C57Bl6 mice were raised in the mouse facility at the Central Institute for the Deaf, in an environment without significant background noise with a 12-h day/night light cycle and fed ad libitum according to the regulations of the Institutional Animal Care and Use Committee at the Washington University School of Medicine. At ages of 10–15 weeks they were randomly assigned to control or LPS experimental groups.

**LPS Treatment.** Mice assigned to the LPS group received 1.0 mg/kg of lipopolysaccharide (Sigma-Aldrich, St. Louis, MO, USA) in sterile saline via intraperitoneal injection for two consecutive days. Daily weights were obtained. Mice lost approximately 5–10 % of their body weight by day 3.

**Fluorescein Administration and Phlebotomy.** On day 3, mice were injected with a 0.5 ml of a 10 mg/ml solution of sodium fluorescein (Sigma, St. Louis, MO, USA) intravenously or intraperitoneally. Sodium fluorescein was dissolved in lactated Ringer's solution. Concentration of serum fluorescein was measured in all animals after perilymph sampling by sampling blood from the internal jugular vein. Two samples of 10 μL of blood were taken from each animal.

**Sequential Sampling from the Posterior SCC of the Mouse.** Mice were anesthetized with ketamine and xylazine IP (80 mg/kg ketamine, 10 mg/kg xylazine). The mouse was tracheostomized and placed in a head holder in the right lateral decubitus position. A heating pad was in place with the temperature set to 36 °C. An incision was made behind the pinna, and the most lateral portion of the posterior SCC was exposed and the bone was cleared of soft tissues. The bone was dried and a thin layer of cyanoacrylate glue applied, followed by layers of two-part silicone (Kwik-Cast, WPI, Sarasota, FL, USA). The silicone was applied thinly over the canal but thicker at the periphery, forming a cup shape as described previously (Salt et al. 2006, 2003). The bone overlying the membranous canal was curetted with a small surgical pick. As clear fluid emerged, it was collected by capillary action into calibrated glass tubes (VWR 53432-706) that were marked for a nominal volume of 0.5 µL. Five to seven samples were collected sequentially, each sample requiring about 15–30 s to accumulate (an efflux rate of ~1–2 µL/min). The length of each sample in the capillary was measured with a calibrated dissecting microscope and each sample was diluted and analyzed independently.

**Fluorescein Measurements.** Perilymph and serum samples were diluted in 100 µL of phosphate-buffered saline. Blood samples were centrifuged at 4,000 RPM for 3 min and the supernatant was loaded onto a 96-well plate alongside the perilymph samples. Reference standards were made by preparing eight serial 10× dilutions of the injected fluorescein solution (10 mg/mL). These were loaded into the same 96-well plate to use as standards and read on a Synergy HT plate reader. The Solver capability of Microsoft Excel was used to fit a Hill function that was fitted to the data acquired from the standards (fluorescence versus fluorescein concentration). This curve was used to transform fluorescence readings to fluorescein concentration for the experimental samples. Perilymph and serum concentrations were calculated based on the specific sample volume and its dilution. Fluorescein concentrations of inner ear fluid were plotted as perilymph fluorescein concentration with respect to serum fluorescein concentration and expressed as a percentage (100×concentration in perilymph/concentration in serum).

**In Vivo Measurement of $Na^+$ Concentration of Inner Ear Fluid.** A separate experiment was conducted on control mice to assess the ion content of the sampled fluid. In order to confirm that our measurements reflected perilymph and not endolymph, we elected to measure ion content of the fluid that emerged from the posterior canal. The sodium concentration of fluids emerging from the perforated posterior semicircular canal was measured using Na-selective electrodes using methods similar to those published (Salt et al. 2006). Briefly, one barrel (the ion sensitive side) of a double-barreled pipette was silanized with dimethyl dichlorosilane vapor, and the tip was beveled to a diameter of ~4 µm. The silanized (ion) barrel was filled with 500 mM NaCl and the nonsilanized (reference) barrel was filled with 500 mM KCl. A small column of sodium-selective ion exchanger (Fluka Sodium Ionophore 1, Cocktail A, 99314) was drawn into the ion barrel. Electrical contact to each barrel was made with Ag/AgCl wires. Readings were made through a custom high impedance ($>10^{14}$ Ω) electrometer, with the sodium-sensitive voltage measured differentially between the ion and reference barrels of the electrode. Electrodes were calibrated in four different standards with mixtures of sodium and potassium, representing solutions that were similar to perilymph, endolymph, and mixtures of both. Standards contained the following:

1. 130 mM Na, 4 mM K (similar to perilymph)
2. 65 Na mM, 82 mM K (1:1 mixture of perilymph and endolymph)
3. 13 mM Na, 144 mM K (1:9 mixture of perilymph and endolymph)
4. 0 mM Na, 160 mM K (similar to endolymph)

Standards were maintained near body temperature in a chamber through which warm water was circulated.

After the electrode was calibrated, the posterior semicircular canal (SCC) was opened. During this portion of the procedure, the electrode was immersed in saline placed in the mouse pinna to keep the electrode conditioned and close to the field. After the semicircular canal was opened, the electrode was quickly moved from the pinna to the droplet of fluid accumulating in the silicone cup overlying the canal. Ion-selective microelectrodes are sensitive to nearby motion and to electrical fields; thus, recordings commenced when the investigator left the chamber and turned off the AC-powered equipment, including the microscope light source. Recordings were deemed to be accurate approximately 30 s after the canal had been perforated.

**TSLIM Imaging and Segmenting Mouse Inner Ear Tissues.** The anatomy and fluid volumes of the mouse inner ear were derived by 3D reconstruction of images of a mouse inner ear obtained by thin-sheet laser imaging microscopy (TSLIM) (Santi et al. 2008). The fixed, decalcified inner ear was dehydrated using a graded ethanol series, stained *en block* with Rhodamine isothiocyanate (1 mg/200 ml of 100 % ethanol) and cleared in Spalteholz solution (5:3 methyl salicylate:benzyl benzoate). The inner ear was attached to a plastic rod and immersed in Spalteholz solution in the TSLIM specimen chamber. TSLIM uses a green laser to project a thin sheet of light through the transparent specimen and the fluorescent planes illuminated by the laser are recorded as optical sections through the tissue (Santi et al. 2009). Movement of the

specimen through the light-sheet nondestructively produces a complete stack of serial sections of the whole cochlea. Each section had a thickness of 10 μm, giving initial voxel dimensions of 2.31×2.31×10 μm.

The Z-stack for the inner ear was loaded into Amira v. 4.1 (Visage Imaging, San Diego, CA, USA) and was down-sampled by a factor of 4 in *X* and *Y* planes, providing a specimen with voxels 9.24×9.24×10 μm that was used for 3D reconstruction of inner ear structures. To isolate different inner ear structures and compute their morphometric characteristics, a process called segmentation was used. Initial segmentation was performed with Amira's semiautomated tools, allowing the borders of each structure to be outlined in a different color in every section of the stack, with the same structures indicated by the same color (shown on Table 1: each color defining designated spaces such as scala tympani, scala vestibuli, etc.). All the soft tissue and fluid spaces within the entire otic capsule were assigned to a structure. Final segmentation was performed manually on a voxel-by-voxel basis, repeated for each of three planes of imaging. Amira provided isosurface volume reconstructions of each inner ear structure segmented and gave a measure of total volume of each structure based on the number of voxels allocated to each structure and the voxel size.

## RESULTS

### Inner Ear Volumes

The volumes of inner ear fluids available from the mouse are substantially lower than from animals typically used to study inner ear fluid pharmacokinetics, such as guinea pigs. Based on a 3D reconstruction of the entire mouse inner ear shown in Figure 1, we estimated that total perilymph volume was 0.96 μL, comprising 0.66 μL from the scala vestibuli and vestibular organs and 0.30 μL from scala tympani (Table 1). Total endolymph volume was estimated to be 0.78 μL, made of 0.30 μL in cochlear endolymph and 0.48 μL in the endolymphatic spaces of the vestibular organs. Volumes associated with tissue spaces of the ear were the following: lateral wall 0.33 μL; neural spaces 0.13 μL; sensory tissues 0.14 μL; and spiral ganglion 0.08 μL. These spaces combine to make the total volume of the mouse ear, including the modiolus, of 2.42 μL. These volumes may differ slightly in the live ear as compared with volumes estimated through the decalcified, dehydrated, cleared mouse specimens.

**TABLE 1**

Inner ear fluid volumes derived from reconstructions of TSLIM data

| | |
|---|---|
| Total fluid volume (μL) | 1.74 |
| Perilymph | 0.96 |
| Scala vestibuli and vestibular perilymph | 0.66 |
| Scala tympani | 0.30 |
| Endolymph | 0.78 |
| Cochlear endolymph | 0.30 |
| Vestibular endolymph | 0.48 |
| Total soft tissue volume | 0.68 |
| Lateral wall (spiral ligament and stria vascularis) | 0.33 |
| Neural spaces (modiolus, spiral ganglion) | 0.21 |
| Sensory epithelium and spiral limbus | 0.14 |
| Total inner ear volume (fluid and soft tissue) | 2.42 |

All the soft tissue and fluid spaces within the otic capsule were designated as part of a named structure in order to generate volume estimates of the mouse inner ear. TSLIM data sent to Washington University by Peter Santi at the University of Minnesota were analyzed and processed using AMIRA software. The total fluid volume of the mouse was 1.74 μL, consisting of 0.96 μL of perilymph and 0.78 μL of endolymph. The soft tissue volume of the inner ear was 0.68 μL. Hence, the volume of fluid is 2.5 times that of the soft tissues in the inner ear. Sampling from the inner ear fluids spaces makes sense when attempting to characterize the permeability of substances from the vascular compartment into the inner ear

### Perilymph from the Perforated Inner Ear: Fluid Collected from the Posterior Canal Represents Vestibular Perilymph, Then Cochlear Perilymph, Then Cerebrospinal Fluid in Sequence

Perforation of the posterior semicircular canal results in fluid efflux (arrow in Fig. 1A) driven by CSF pressure transmitted to the inner ear fluid via the cochlear aqueduct. This results in cerebrospinal fluid entry into the inner ear at the base of the scala tympani (ST), with apical flow in ST towards the helicotrema, basally directed flow in the scala vestibuli (SV) and flow through the vestibule to the perilymphatic spaces of the semicircular canals (SCCs) as illustrated in Figure 1B. The first sample, which measured approximately 0.5 μL, collected from the posterior semicircular canal consisted of the vestibular perilymph according to our measured fluid volumes. The second sample represented perilymph from SV and ST that had passed through the vestibule and SCCs. Later samples consisted of CSF that had passed through the fluid spaces of the ear before emerging at the fenestration site. Thus, the first two samples represented fluid from the inner ear, the first sample from the vestibular organs and the second from the cochlea, and the third and subsequent samples originated from the cerebrospinal fluid almost exclusively. Although this pattern of inner ear fluid flow was established in guinea pigs, the cochlear and vestibular anatomy of the mouse supports a similar interpretation (Salt and Stopp 1979; Salt et al. 2012).

### Fluorescein in Inner Ear Fluids: LPS Compromises the BLB

We administered sodium fluorescein via intravenous or intraperitoneal injections. Fluorescein entered the

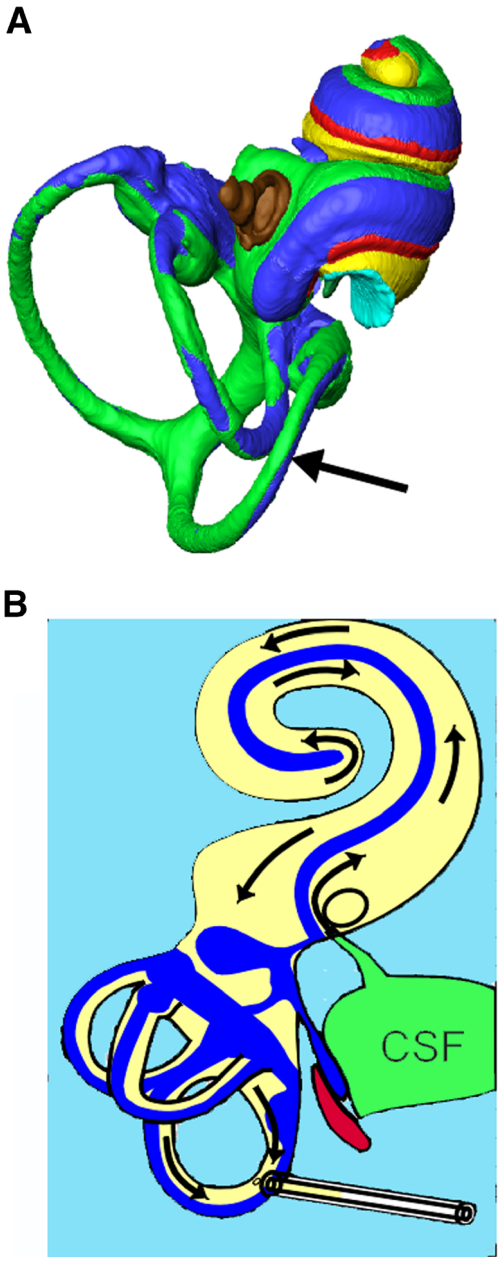


**FIG. 1.** Anatomic schematic diagram of inner ear and fluid compartments sampled. **A** Reconstructed inner ear fluid spaces of the mouse with the site of perilymph sampling at the posterior semicircular canal are shown. The bone of the otic capsule has been removed as well as the lateral wall. (Color key: *Green*: perilymph in scala vestibuli and vestibular organs; *Yellow*: perilymph in scala tympani; *Red*: sensory structures; *Blue*: endolymph; *Brown*: stapes. *Arrow* points to the fenestration site in the posterior canal.) **B** Flow diagram of inner ear fluids during sampling: path of fluid movement when the posterior canal is perforated. Perilymph is displaced by cerebrospinal fluid (CSF) entering through the cochlear aqueduct, causing flow towards the apex in scala tympani, connecting through the helicotrema to the scala vestibule, towards the base in scala vestibuli and passing through the vestibule to exit at the lateral semicircular canal. Multiple samples of 0.5 µL volume were collected sequentially. As perilymph volume was estimated to be approximately 0.96 µL, the first two samples contained mostly perilymph and later samples contained CSF that had passed through the perilymph spaces.

vascular space immediately with both routes of administration, and the mice showed signs of fluorescein uptake through yellow discoloration of the mucosa and fluorescent yellow tears and urine within 5 min of injection. Serum concentrations of fluorescein were high and varied over a large range (80–450 µg/mL). There was no statistically significant difference in serum levels of fluorescein when we compared control animals with LPS-treated animals (Mann-Whitney $U$ test $p$=0.074). Fluid collected from the inner ear was clear and showed no indication of contamination with erythrocytes. The inner ear fluids demonstrated fluorescein concentrations considerably below those of the serum, ranging from 0.2 to 78 µg/mL. The inner ear fluid samples were collected 30–40 min after the initial fluorescein injection. A time course of fluorescein uptake was performed as an initial experiment, and we found that serum levels reached a peak by 60 min post-injection and remained flat to 90 min post-injection. By 30 min post-injection, mice demonstrated serum levels that were 70–95 % of their peak values. All inner ear fluorescein measurements are reported here as percent of serum levels, thus normalizing for differences between animals in serum concentrations of fluorescein. Here, we report the inner ear fluid and serum concentrations of fluorescein in five controls and eight LPS-treated mice.

Fluorescein concentrations in the inner ear have been expressed as a percentage, normalized to the fluorescein concentration in the serum at the time of sampling. Figure 2 demonstrates the concentration of fluorescein in the inner ear relative to that in the serum expressed as a percentage for each mouse with 5–7 sequential samples drawn from the inner ear of each animal. We consider this measurement as indicative of vascular permeability, where 100 % would indicate that the concentration of fluorescein in the inner ear and in the serum are equal, and no barrier is present at the time of measurement, while values lower than 100 % would indicate that a barrier is present between the intravascular fluids and the inner ear fluids with varying degrees of porosity. Values greater than 100 % would suggest an active pumping mechanism into the inner ear or a barrier in the opposite direction, impeding resorption of fluorescein back into the bloodstream. As sample volumes varied slightly from experiment to experiment, the fluorescein ratios are plotted against the total accumulated volume, in microliters. On the basis of the volume collected, we can estimate the origin of the fluid, e.g., vestibular or cochlear, inner ear, or CSF.

Figure 3 shows fluorescein percentages (inner ear concentration divided by serum concentration) as

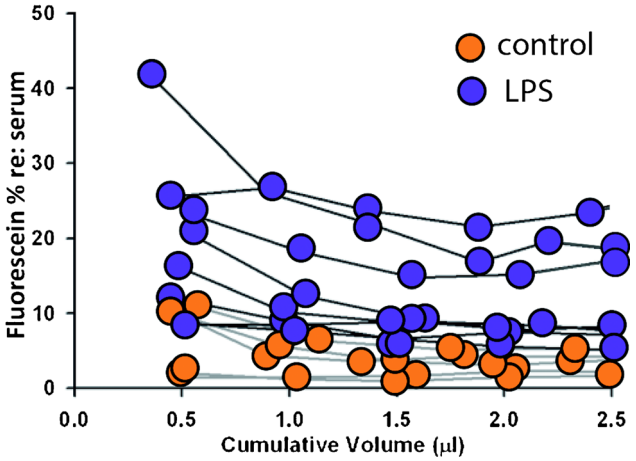


**FIG. 2.** Fluorescein percent is higher in inner ear fluid of LPS-treated mice compared with controls. Fluorescein concentrations were normalized to serum concentration and plotted against the cumulative volume that was collected from each ear following perforation of the posterior SCC. Five control mice and eight LPS-treated mice were tested for inner ear fluid fluorescein content. The range of values for the initial sample for control mice was 1–11 % and for LPS treated mice was 8–42 %. In later samples containing CSF (after 1 µL), the control fluorescein percentages ranged from 2–4 %, while LPS-treated mice ranged from 5–24 %.

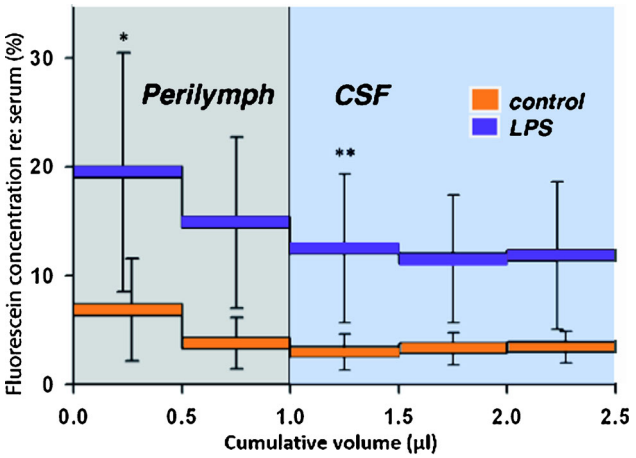


**FIG. 3.** Inner ear fluid contains higher percentages of fluorescein in LPS-treated mice when compared with control mice. Averaged fluorescein concentrations for eight LPS-treated and five control animals. *Error bars* show standard deviation. The percent of fluorescein recovered from inner ear samples when compared with serum levels in each experimental mouse showed that mice pretreated with LPS had larger fluorescein percentages when compared with that of controls. The higher concentration of fluorescein found in LPS-treated mice were highly significant (mixed model ANOVA, $p<0.001$) The *orange* and *purple horizontal bars* represent the average inner ear fluorescein concentration for the first 500 nL, second 500 nL, etc. The *gray-shaded box* represents the approximate volume of perilymph, so that the first sample contains perilymph from the vestibule and part of scala vestibuli, and the second sample contains perilymph originating from the apical part of scala vestibuli and from scala tympani. Subsequent samples (cumulative volume greater than 1.0, *blue area*) contain CSF that has flowed into the inner ear and replaced the perilymph. Statistical analysis using a mixed model analysis ANOVA also showed a significant difference between sample 1 (*first bar*) and sample 3 (*third bar*, <0.001), suggesting that Na fluorescein entry properties are different in perilymph versus CSF.

group averages, with orange demonstrating average fluorescein percentages for inner ear fluids in control mice and purple representing average fluorescein percentages for LPS-treated mice. The first two bars represent fluorescein concentrations in the inner ear (roughly, vestibular perilymph in the first bar and cochlear perilymph in the second bar), and the third and subsequent bars reflect the fluorescein percentage in the cerebrospinal fluid that has passed through the ear before collection.

This graph shows significantly higher percentages of fluorescein in the perilymph of LPS-treated mice compared to controls. The difference in the percent fluorescein in perilymph of control mice compared to percent fluorescein in LPS-treated mice was statistically significant (mixed model analysis with autoregressive structure $F=5.4$; $p=0.04$). Thus, we believe that like the blood-brain barrier, the blood-labyrinth barrier is disrupted as a result of LPS treatment, and entry of fluorescein into the inner ear fluids from the vasculature is increased as a result of systemic inflammation. It is apparent from samples 3, 4, and 5 that LPS-treated animals demonstrate higher levels of fluorescein entry into the CSF as well as into the perilymph when compared to controls.

Additionally, we observed that the blood-labyrinth barrier does not completely prevent fluorescein entry into the mouse perilymph in control mice. There is a low level of fluorescein that enters the perilymph of normal mice. Thus, if there were a condition in which BLB permeability were further reduced compared to normal mice, this technique could be used to measure such a change.

In both groups, fluorescein percentages were higher in perilymph samples than in samples containing CSF. These data suggest that fluorescein collects in the perilymph more quickly than in the cerebrospinal fluid. In both groups of animals, the first sample, originating from vestibular perilymph, had a higher concentration of fluorescein than the second sample, and the second sample, arising from cochlear perilymph, demonstrated an intermediate level of fluorescein concentration, while CSF demonstrated the lowest concentration when compared to the two samples from the inner ear. This difference in fluorescein uptake into the various fluid compartments could be explained in part by the kinetics of solute entry into the two respective fluid spaces. The ratio of the total surface area of feeding blood vessels to the volume of fluid primarily determines the rate of fluorescein entry into perilymph and CSF. The rate of CSF secretion and resorption would also affect the

rate of entry of fluorescein into the subarachnoid space. Thus, the difference between inner ear and CSF fluorescein concentration might reflect differences in the density of the vasculature and the total volume of perilymph and CSF, not necessarily a difference in endothelial permeability.

### $Na^+$ ion Measurement: The Sampled Fluid Consists of Perilymph

In order to evaluate the integrity of the blood-perilymph barrier, it was vitally important to confirm that our samples contained perilymph and not endolymph. Compared to perilymph, the endolymph environment is even more strictly regulated. Changes in vascular permeability of the inner ear would affect the perilymph more readily than the endolymph, and substantive changes in the barrier might be missed if we were sampling endolymph believing this to be perilymph. Because the semicircular canals contain predominantly endolymph, we were compelled to confirm that the sampled fluid was indeed perilymph. The space occupied by perilymph within the canals is small and collapsed, with the membranous labyrinth being adherent to the endosteum in some regions within the semicircular canals. However, the collected volumes recorded here far exceed the total volume of mouse endolymph.

Thus, we measured the ion content of the sampled fluid to ascertain its composition. We initially attempted to measure potassium concentration of the collected fluid samples, but in four experiments with two different potassium exchangers, potassium measures were erratic and consistently too high (above 500 mM), which we believed to be due to interference from another ion, possibly ammonium ($NH_4^+$) in the mouse inner ear fluids. We therefore elected to measure the sodium concentration [$Na^+$] in the droplet that collected from the perforated SCC using a double-barrel, ion-sensitive electrode and followed this concentration over time during fluid collection after perforation of the posterior SCC. Figure 4A shows the average [$Na^+$] from eight different mice measured over time in the fluid that collected following the initial perforation. We observed an initial period of instability after the lights in the chamber were extinguished and the door was closed, which is typical for high-impedance ion-selective electrodes. Subsequent measures of sodium levels were stable and high (ranging from 135–165 mM). An almost identical time course was observed when the first droplet was wicked away, and the sodium measurement made in a second fluid droplet that subsequently collected (Fig. 4B). As [$Na^+$] of the second droplet would be dominated by CSF that has passed through the ear, these measurements demonstrate that the initial droplet had [$Na^+$] consistent with accumulation of a high sodium fluid, i.e., completely perilymph. We calculated the concentration time course that would have occurred if the perforation had resulted in efflux of a small volume of endolymph, which was subsequently summed with an increasing volume of high [$Na^+$] solution (perilymph or CSF). The calculations assumed a volume accumulation rate of 1 µL/min with a variable volume (50–500 nL) of zero [$Na^+$] fluid ($V_e$), followed by high [$Na^+$] (140 mM) fluid ($V_p$). Concentrations were calculated as $140 \times V_p / (V_p + V_e)$ for the volumes accumulated at each time point. The calculations show that a rising time course would be expected, depending on the original volume of endolymph contributing to the droplet (Fig. 4C). Based on this calculation, we expect that even 50 nL of endolymph contributing to the droplet could have been detected. When collected as individual samples, rather than accumulating as a single droplet during this measurement, this means that less than 10 % of the initial 0.5 µL sample could be endolymph. The observation that sodium concentration did not show a rising time course and was in the 140-mM range, therefore supports the view that the samples consisted of perilymph initially, and CSF in the later specimens.

Mouse inner ears were harvested after the experiment, and after decalcification and plastic embedding, we performed serial sections of eight temporal bone specimens to examine the site of the fenestration. These histologic sections showed that the surgical opening into the bony canal measured between 50 and 100 µm in diameter. Morphology of the canal at the perforation site showed collapse of the endolymph compartment, separation of the membranous labyrinth from the endosteum of the otic capsule, but no apparent rupture of the endolymphatic boundary near the surgical fenestra in any of the eight temporal bones that were studied. Figure 5 shows an example of one of the temporal bones at the site of the surgical fenestra. We are satisfied that the pick used to fenestrate the bony canal was too blunt to perforate the membranous canal and that the endolymphatic space appeared intact on histologic examination in the ears that were examined.

## DISCUSSION

### The Blood-Labyrinth Barrier Is a Specialized Trait of the Endothelial Bed of the Inner Ear Capable of Separating Small Molecules in the Vascular Compartment from the Inner Ear Fluid Compartment

In these studies, we used perilymph sampling from the semicircular canals to evaluate the function of the blood-labyrinth barrier (BLB) in live mice. In vivo, sodium fluorescein enters the perilymph through the capillary walls of the inner ear vasculature at a slow rate.

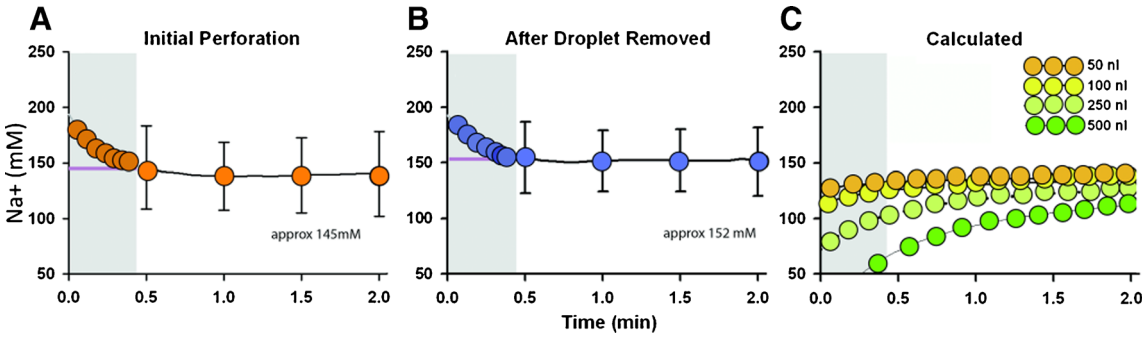


**FIG. 4.** Na-selective electrodes indicate that the inner ear fluid sampled is perilymph. **A** Average [$Na^+$] measured over time in the accumulated droplet following perforation of the posterior semicircular canal. Due to the time required to place the ion-sensitive electrode into emerging fluid droplet, recordings commenced approximately 30 s after canal perforation (shown as zero time on the plots). The first 30 s of the recordings (shown in *gray*) contained artifact as the ion electrode stabilized in solution. From 30 s onward, the average [$Na^+$] measured approximately 145 mM. **B** Average [$Na^+$] measured with time when the initial droplet was removed and a second droplet allowed to accumulate. [$Na^+$] remained high over the next few minutes at which time inner ear fluid was replaced by CSF. **C** Calculated time courses of [$Na^+$] when an initial volume ranging from 50 to 500 nL of low Na fluid (i.e., endolymph) was mixed with high [$Na^+$] fluid (i.e., perilymph or CSF). The initial 30 s of the calculated curves were excluded so that the calculated curves were comparable to the recorded data. If even 50 nL of the initial sample were endolymph, we would have expected to see a rising time course as the initial low Na concentration was progressively combined with perilymph and CSF. The measured data in Figure 5A and B showed no indication of a rising time course, confirming that the initial sample was predominantly perilymph.

The gradient between serum and perilymph and serum and CSF was always in favor of a higher concentration of fluorescein in the serum. Perilymph fluorescein concentrations reached 4–10 % of the plasma level after 30 min in control mice (Fig. 2). The slow entry of fluorescein is comparable to prior studies with small tracer molecules. Fregni and Poli (1954) also used fluorescein to study BLB and BBB permeability in guinea pigs and found entry could be manipulated by experimental treatments such as electrical shocks and vasoactive reagents. Choo and Tabowitz (1964) measured $^{22}Na$ entry into perilymph in cats and found perilymph levels of 3–21 % of plasma concentration after 2 h. Juhn and Rybak (1981) compared entry of a variety of substances in chinchillas, finding even the most permeable (urea and glucose) reached less than 40 % of the plasma level after 1 h. Inamura and Salt (1992) measured entry of the marker tetramethylphenylammonium (TMPA) in guinea pigs, finding that TMPA entered perilymph more slowly than CSF, reaching only ~5 % of the plasma level in 90 min. Hahn et al. showed that perilymph levels of gentamicin, occurring in the apical regions, were only ~14 % of the plasma concentration at 3 h and ~25–33 % of the plasma concentration after 5 h (Hahn et al. 2013). The observation that small molecules enter the perilymph slowly confirms the existence of a barrier between the serum and perilymph. Although previous studies found entry of small molecules occurs more slowly into perilymph than into CSF, we have found fluorescein to enter perilymph more rapidly than CSF (Fig. 3). This is in agreement with the original fluorescein studies in guinea pigs by Fregni and Poli (1954).

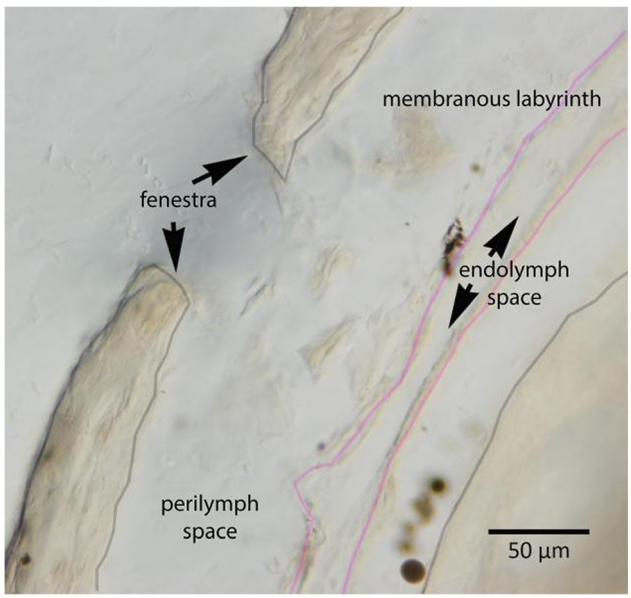


**FIG. 5.** Histology of the mouse posterior semicircular canal. After fluid sampling, mouse petrous bones were harvested, fixed, embedded in plastic, and sectioned. Where the fenestra was created in the posterior canal, serial sections were examined. The bony otic capsule has been entered where "fenestra" is marked, and bone fragments are present just inside the fenestra. The membranous labyrinth had separated from the endosteum and perilymph had filled this potential space. The membranous labyrinth appeared intact in this specimen and in all the specimens examined. The *gray lines* mark the bony structures; the pink lines delineate the membranous compartment. *Scale bar*: 50 µm.

## The Role of Histology in Assessment of the Blood-Labyrinth Barrier

In other studies, the integrity of the BLB has been assessed using histological methods. Sodium fluores-

cein is not a good marker for histological purposes as it remains mobile during histologic processing and becomes evenly distributed throughout the tissues. Rather, larger molecular weight reagents such as Evans blue, radioactive albumin and fluorescent-IgG have been used (Tachibana et al. 1981; Kastenbauer et al. 2001; Trune 1997). Others have measured the dye content of tissue homogenates, but this application in assessment of inner ear vascular permeability has been met with limited success (Rossner and Tempel 1966; Veszelka et al. 2003; Awad 2006). When used in the inner ear, these techniques demonstrate shortcomings due to high levels of contamination from dyes that leach out of the cochlear vessels during tissue processing. Also, the subjective nature of the quantitation is apparent when fluorescent imaging of tissue sections is used to assess for leakage of dye out of vessels in histologic sections (Kastenbauer et al. 2001). The slow entry of small molecules such as TMPA or $^{22}$Na into perilymph is not compatible with early theories that perilymph was formed as an ultrafiltrate of plasma (Schnieder 1974; Zou et al. 2003). In some studies, the presence of fenestrated capillaries have been reported (Jahnke 1980), but the physiological significance of such morphologic observations is uncertain, and the presence of large gradients between in the serum levels and inner ear levels of proteins and other solutes would argue against the presence of such fenestrated capillaries in the inner ear. Furthermore, the presence of certain proteins and solutes that is at higher concentrations in the inner ear fluids than in the serum suggests that the fluid of the inner ear is actively secreted and not a passive ultrafiltrate (Thalmann et al. 1992).

Others have applied histologic analyses focused on endothelial cells in fixed cochlear tissues of the stria vascularis to assess the integrity of blood-labyrinth barrier (Zhang et al. 2012; Shi 2010). In vitro techniques using cell populations to mimic the vasculature of the inner ear, modeled after studies of the BBB, have been used to study the blood-perilymph barrier (Neng et al. 2013). However, we do not know how functional impairment of the barrier correlates to histologic changes or to in vitro findings, as there have been no studies clearly linking these changes to endocochlear potential, ion concentrations or hearing thresholds. Furthermore, our experiments do not test the integrity of the barrier between strial vessels and the intrastrial fluid and are not designed to resolve questions regarding permeability changes of strial vessels, which is the subject of the papers above. This barrier could be more specifically described as the blood-strial barrier, as it does not represent the interface between blood and perilymph. Similarly, our studies do not assess the interface between blood and endolymph, which represents yet another layer of separation from the blood-perilymph barrier.

Intravascular injection of beads or particles such as cationic polyethyleneimine (PEI) has been used in conjunction with transmission electron microscopy to study vascular permeability in the inner ear (Suzuki and Kaga 1999; Suzuki et al. 1998). These studies provide a rigorous method to detect small molecule leakage from specific vessels at high resolution. Nonetheless, while electron microscopy provides excellent subcellular localization of particle leakage, these studies are not quantitative and cannot provide a overview of how gradients between serum and perilymph have changed overall.

## CSF Contribution to Inner Ear Fluids: Sampling from the Semicircular Canal Minimizes Mixing of CSF with Perilymph

The method of perilymph sampling presented here relies on the fact that perforation of the otic capsule releases perilymph pressure resulting in influx of CSF into the scala tympani through the cochlear aqueduct, which subsequently displaces the perilymph contents through the surgical opening in the canal. When perilymph is sampled from scala tympani, CSF contamination is certain and will prevent collection of pure perilymph samples; therefore, we avoid sampling from this area (Salt et al. 2003). In the present study, the site of perilymph efflux is as far as possible from the cochlear aqueduct so that virtually all perilymph is displaced before CSF reaches the efflux site. When taken as small aliquots, this method ensures that all perilymph is collected before CSF reaches the semicircular canals. Because these fluid-filled structures between the aqueduct in the base of scala tympani and the collection site in the posterior canal are tortuous, fine-diameter tubes, consisting of scala tympani, scala vestibuli, and the vestibule, fluids cannot easily intermix or be stirred during the collection procedure. The interscalar communication between scala tympani and scala vestibuli across the spiral ligament occurs slowly relative to the rate of perilymph displacement such that this soft tissue communication does not play a major role in mixing of fluids. Based on the perilymph volume of the mouse, the first two samples collected are perilymph with minimal CSF contamination. Later samples are dominated by CSF that has passed through the perilymphatic spaces and are collected in order to assess the BBB and to provide a comparison of the permeability of the BLB.

## Functional Barrier Properties Are Revealed by Perilymph Sampling, Specific Anatomic Location Is Not

Perilymph sampling after systemic fluorescein injection provides little indication of where the breaches in the BLB are occurring or what cells are involved in permeability changes. Nevertheless, if perilymph composition is disturbed due to a pathological process, the change in perilymph chemistry and the physiologic changes associated with this breach are the keys to understanding functional changes that could be caused by compromise of the BLB. Indeed, it is currently unknown if hearing function is directly affected by the integrity of the BLB. Using this quantitative assessment of permeability changes, we can test whether thresholds or endocochlear potential are affected when the BLB is altered, and what degree of BLB compromise could cause a change in threshold. These data complement anatomic studies of the barrier and provide different information that is essential to improve our understanding of the interaction between inner ear function and inner ear vascular permeability. The vessels that travel through tissues that are bathed in perilymph all contribute to fluorescein leakage into perilymph. These vessels include those of the spiral ligament, spiral limbus, modiolus, and stroma underlying the vestibular sensory epithelium. The fluorescein content of perilymph does not assess the integrity of the strial vessels because compromise of the tight junctions in strial vessels would result in fluorescein leakage into the intrastrial space, which is separated and contained from the perilymph, and was not sampled in these experiments. It is possible that fluorescein leakage into the perilymph could contribute in small part to leakage into the intrastrial space or the endolymph, but this would require passage through another set of barriers beyond the perilymph compartment. Despite our inability to assess the specific location of leaky vessels, we were able to quantify the percent of fluorescein entering the inner ear with respect to serum, the time course of the effect and provide a comparison to changes in the CSF entry. These changes in kinetic properties cannot be derived from histological assessments of the boundaries.

## Systemic Inflammation Induced by LPS Causes Compromise of the BLB

These experiments demonstrate definitively that systemic inflammation induced by LPS compromises the blood-labyrinth barrier. We have proven this by measuring perilymph concentration of fluorescein originating from the serum. Fluorescein is an anion with a molecular weight of 376 and is small enough to enter the perilymph at a low level in control mice. The passage of fluorescein from vessels into perilymph occurs more quickly and to higher concentrations after LPS treatment when compared with saline-treated controls. It is likely that LPS causes permeability changes in the BLB using pathways similar to those affecting the blood-brain barrier (BBB). The BBB has been shown to be vulnerable to potent inflammatory stimuli such as LPS. In studies of the BBB, LPS binds Toll-like receptor 4 (TLR4) on leukocyte and endothelial cell surfaces, which results in the production of inflammatory cytokines, among them, TNF-alpha. Subsequent activation of myeloid differentiation factor 88 (MyD88) plays a critical role in the downstream effects of LPS, with resultant loss of endothelial tight junction integrity within endothelial cells of the brain (McGettrick and O'Neill 2010; Tauseef et al. 2012; Wang et al. 2011; Zhou et al. 2006). These effector molecules activated by inflammation are relatively understudied elements of inner ear dysfunction. Mononuclear phagocyte migration into the inner ear, which has been observed in inner ear injury, could play an important role in hearing and balance dysfunction and is accompanied by other inflammatory mediators that affect the short and long term function of the inner ear in the disease state (Hirose et al. 2005; Sato et al. 2010). In many organ systems, inflammation is accompanied by changes in vascular permeability, and LPS is only one of many ways to stimulate local or systemic inflammation. Other forms of inner ear injury, such as acoustic trauma, induce monocyte and macrophage migration into the cochlea. In the past, noise injury has been proposed to cause changes in vascular permeability in the inner ear although evidence to support this concept has been sparse. Such hypotheses can now be tested using this functional technique, providing a method to assess BLB permeability as a result of metabolic or other perturbations.

## Differences in Fluorescein Content Comparing Perilymph to CSF: Not Necessarily an Indication of Higher Permeability of the Inner Ear Compared to the Brain but of Vascular Density

In this experimental protocol, we sampled both perilymph and cerebrospinal fluid from each mouse. The first microliter of fluid removed from the posterior semicircular canal consisted nearly completely of perilymph while the subsequent fluid samples, which consisted of another two to three microliters of fluid, contained CSF. As expected, the fluorescein percentage present in the CSF was also higher in LPS pretreated mice than in control mice. These findings are consistent with other studies that demonstrate compromise of the blood-brain barrier

in LPS-pretreated animals (Jangula and Murphy 2013; Wispelwey et al. 1988; Cardona et al. 2008). A compromised blood-brain barrier has also been found in animals with experimental models of multiple sclerosis and in infectious conditions of the brain and spinal cord (Nadeau and Rivest 2002; Wispelwey et al. 1988; Charlier et al. 2009; Lustig et al. 1992; McCandless et al. 2008; Diamond and Klein 2004). The difference between fluorescein content in the perilymph versus that in the CSF may be reflecting the fact that there is a higher volume of CSF than perilymph and therefore a more diluted pool of fluorescein, and that there are a greater density of vessels in contact with perilymph than there are vessels in contact with CSF. The difference in fluorescein percent in these two different spaces does not necessarily reflect a difference in barrier permeability.

### Differences in Fluorescein Content in Vestibular Versus Cochlear Fluids

With respect to the gradients of fluorescein concentration among the various fluid samples taken from the inner ear, the initial sample, which consisted of 0.5 μL of perilymph from vestibular organs and scala vestibuli, demonstrated the highest concentration of fluorescein. The second 0.5 μL demonstrated a lower fluorescein percentage when compared to vestibular perilymph. CSF samples showed the lowest fluorescein percent when normalized to serum levels of fluorescein. This difference could reflect a higher permeability of the blood-labyrinth barrier in the vestibular perilymph than in cochlear perilymph. These data also suggest that fluorescein entry kinetics are not homogeneous throughout the ear, and that entry kinetics into the ear are different from those into CSF. The second sample that had a lower fluorescein percent than the first could be lower due to faster entry of fluorescein into scala vestibuli and the vestibule than into scala tympani. A lower concentration in scala tympani could also result from physiological entry of CSF into the basal turn of the mouse cochlea comparable to that found in guinea pig (Salt et al. 2012). At present, the degree to which CSF enters the mouse cochlea under conditions where the otic capsule is not perforated is unknown.

Careful measurements of mouse inner ear structures reveal that total perilymph volume is 0.96 μL. Thus, we can conclude that the first two 0.5 μL samples originate almost exclusively from inner ear fluids and not CSF. We are currently in the process of incorporating the spatial anatomy of the fluid and tissue spaces of the mouse anatomy into a simulation program that will allow more detailed interpretation of sampling experiments, comparable to those that have been performed in the guinea pig (Salt et al. 2006). This analysis incorporates the interactions between fluid and tissue spaces as the fluids flow through the ear during collection. As the fluid flow rate in the mouse is high, the contributions of fluid-tissue interactions are likely small.

### The Fluid Sampled in These Experiments Is Perilymph, Not Endolymph

The semicircular canals contain a greater volume of endolymph than perilymph, and we were concerned about possible contamination of our inner ear fluid samples with endolymph during these experiments, providing a falsely low reading of fluorescein concentration. In the mouse compared to other species, the endolymph volume is large relative to perilymph volume. From prior work by Thorne et al., endolymph to perilymph ratios in the cochlea were 1:7 in guinea pig and 1:3 in mouse (Thorne et al. 1999). These measurements were performed using the cochlea only, not the vestibular organs, where an even larger percentage of the fluid consists of endolymph. Because of the high volume of endolymph in the semicircular canals, and the membranous labyrinth being in close contact with the endosteum of the semicircular canals, we elected to measure the ion content of the fluid to ascertain its source. Because the total endolymph volume in a mouse is small (0.78 μL), compared to the total volume that was collected (over 2.5 μL), the collected fluid could not have been exclusively endolymph and is certainly dominated by CSF towards the end of the sampling period. Nevertheless, the possibility existed that some portion of the initial sample could have been endolymph, which was subsequently diluted with perilymph and CSF. Measurements of sodium concentration of the fluid emerging from the SCC were obtained and on average showed a concentration of 145 mM, which is consistent with perilymph alone. Furthermore, the changes in sodium concentration over time were not consistent with contamination of perilymph with endolymph. Histologic sections of the semicircular canals demonstrated that the membranous labyrinth at the posterior semicircular canal fenestration site appeared intact. Thus, we feel that we can conclude that samples obtained using this method are comprised of perilymph and CSF.

## ACKNOWLEDGMENTS

Many thanks to Ruth Gill for her fine work in analyzing the TSLIM data and segmenting the 3D structures to estimate fluid volumes. Thanks to Song-Zhe Li who provided care for

the mice and performed LPS and saline pretreatment. Also, thank you to Kevin Ohlemiller for thoughtful critique of the experiments and the manuscript, and to Dorina Kallojieri for her assistance with the statistical analysis.

*Conflict of Interest* None of the authors who have authored or provided materials for this work have a financial, personal, or other conflicting interest in the results of this research or publication of this work.

## REFERENCES


AWAD AS (2006) Role of AT1 receptors in permeability of the blood-brain barrier in diabetic hypertensive rats. Vasc Pharmacol 45(3):141–147. doi:10.1016/j.vph.2006.04.004

CARDONA AE, LI M, LIU L, SAVARIN C, RANSOHOFF RM (2008) Chemokines in and out of the central nervous system: much more than chemotaxis and inflammation. J Leukoc Biol 84(3):587–594. doi:10.1189/jlb.1107763

CHARLIER C, NIELSEN K, DAOU S, BRIGITTE M, CHRETIEN F, DROMER F (2009) Evidence of a role for monocytes in dissemination and brain invasion by *Cryptococcus neoformans*. Infect Immun 77(1):120–127. doi:10.1128/IAI.01065-08

CHOO YB, TABOWITZ D (1964) The formation and flow of the cochlear fluids. I. Studies with radioactive sodium (Na22). Ann Otol Rhinol Laryngol 73:92–100

DANEMAN R, ZHOU L, KEBEDE AA, BARRES BA (2010) Pericytes are required for blood-brain barrier integrity during embryogenesis. Nature 468(7323):562–566. doi:10.1038/nature09513

DIAMOND MS, KLEIN RS (2004) West Nile virus: crossing the blood-brain barrier. Nat Med 10(12):1294–1295. doi:10.1038/nm1204-1294

ENGELHARDT B, RANSOHOFF RM (2012) Capture, crawl, cross: the T cell code to breach the blood-brain barriers. Trends Immunol 33(12):579–589. doi:10.1016/j.it.2012.07.004

FERNANDEZ-LOPEZ D, FAUSTINO J, DANEMAN R, ZHOU L, LEE SY, DERUGIN N, WENDLAND MF, VEXLER ZS (2012) Blood-brain barrier permeability is increased after acute adult stroke but not neonatal stroke in the rat. J Neurosci : Off J Soc Neurosci 32(28):9588–9600. doi:10.1523/JNEUROSCI.5977-11.2012

FREGNI R, POLI A (1954) Convulsive state produced by various types of shock, conduct of three barriers (blood-aqueous, blood-labyrinthine fluids, and blood-liquor [spinal fluid]) with reference to some convulsive states. J Am Med Assoc; Arch Otolaryngol 60(2):149–153

HAHN H, SALT AN, SCHUMACHER U, PLONTKE SK (2013) Gentamicin concentration gradients in scala tympani perilymph following systemic applications. Audiol Neuro-Otol 18(6):383–391. doi:10.1159/000355283

HARA A, SALT AN, THALMANN R (1989) Perilymph composition in scala tympani of the cochlea: influence of cerebrospinal fluid. Hear Res 42(2–3):265–271

HE Z, WANG X, WU Y, JIA J, HU Y, YANG X, LI J, FAN M, ZHANG L, GUO J, LEUNG MC (2014) Treadmill pre-training ameliorates brain edema in ischemic stroke via down-regulation of aquaporin-4: an MRI study in rats. PLoS One 9(1):e84602. doi:10.1371/journal.pone.0084602

HIROSE K, DISCOLO CM, KEASLER JR, RANSOHOFF R (2005) Mononuclear phagocytes migrate into the murine cochlea after acoustic trauma. J Comp Neurol 489(2):180–194

HOLMAN DW, KLEIN RS, RANSOHOFF RM (2011) The blood-brain barrier, chemokines and multiple sclerosis. Biochim Biophys Acta 1812(2):220–230. doi:10.1016/j.bbadis.2010.07.019

INAMURA N, SALT AN (1992) Permeability changes of the blood-labyrinth barrier measured in vivo during experimental treatments. Hear Res 61(1–2):12–18

JAHNKE K (1980) The fine structure of the cochlear plexus. Arch Otorhinolaryngol 228(3):155–161

JANGULA A, MURPHY EJ (2013) Lipopolysaccharide-induced blood brain barrier permeability is enhanced by alpha-synuclein expression. Neurosci Lett 551:23–27. doi:10.1016/j.neulet.2013.06.058

JUHN SK, RYBAK LP (1981) Labyrinthine barriers and cochlear homeostasis. Acta Otolaryngol 91(5–6):529–534

JUHN SK, RYBAK LP, FOWLKS WL (1982) Transport characteristics of the blood—perilymph barrier. Am J Otolaryngol 3(6):392–396

KASTENBAUER S, KLEIN M, KOEDEL U, PFISTER HW (2001) Reactive nitrogen species contribute to blood–labyrinth barrier disruption in suppurative labyrinthitis complicating experimental pneumococcal meningitis in the rat. Brain Res 904(2):208–217

LUSTIG S, DANENBERG HD, KAFRI Y, KOBILER D, BEN-NATHAN D (1992) Viral neuroinvasion and encephalitis induced by lipopolysaccharide and its mediators. J Exp Med 176(3):707–712

MCCANDLESS EE, ZHANG B, DIAMOND MS, KLEIN RS (2008) CXCR4 antagonism increases T cell trafficking in the central nervous system and improves survival from West Nile virus encephalitis. Proc Natl Acad Sci U S A 105(32):11270–11275. doi:10.1073/pnas.0800898105

MCGETTRICK AF, O'NEILL LA (2010) Regulators of TLR4 signaling by endotoxins. Subcell Biochem 53:153–171. doi:10.1007/978-90-481-9078-2_7

NADEAU S, RIVEST S (2002) Endotoxemia prevents the cerebral inflammatory wave induced by intraparenchymal lipopolysaccharide injection: role of glucocorticoids and CD14. J Immunol 169(6):3370–3381

NENG L, ZHANG W, HASSAN A, ZEMLA M, KACHELMEIER A, FRIDBERGER A, AUER M, SHI X (2013) Isolation and culture of endothelial cells, pericytes and perivascular resident macrophage-like melanocytes from the young mouse ear. Nat Protoc 8(4):709–720. doi:10.1038/nprot.2013.033

NISHIOKU T, DOHGU S, TAKATA F, ETO T, ISHIKAWA N, KODAMA KB, NAKAGAWA S, YAMAUCHI A, KATAOKA Y (2009) Detachment of brain pericytes from the basal lamina is involved in disruption of the blood-brain barrier caused by lipopolysaccharide-induced sepsis in mice. Cell Mol Neurobiol 29(3):309–316. doi:10.1007/s10571-008-9322-x

ROSSNER W, TEMPEL K (1966) Quantitative determination of the permeability of the so-called blood-brain barrier of Evans blue (T 1824). Med Pharmacol Exp Int J Exp Med 14(2):169–182

SALT AN, STOPP PE (1979) The effect of cerebrospinal fluid pressure on perilymphatic flow in the opened cochlea. Acta Otolaryngol 88(3–4):198–202

SALT AN, KELLNER C, HALE S (2003) Contamination of perilymph sampled from the basal cochlear turn with cerebrospinal fluid. Hear Res 182(1–2):24–33

SALT AN, HALE SA, PLONKTE SK (2006) Perilymph sampling from the cochlear apex: a reliable method to obtain higher purity perilymph samples from scala tympani. J Neurosci Methods 153(1):121–129. doi:10.1016/j.jneumeth.2005.10.008

SALT AN, HARTSOCK JJ, GILL RM, PIU F, PLONKTE SK (2012) Perilymph pharmacokinetics of markers and dexamethasone aplied and sampled at the lateral semi-circular canal. J Assoc Res Otolaryngology : JARO 13(6):771–783

SANTI P, RAPSON I, VOIE A (2008) Development of the mouse cochlea database (MCD). Hear Res 243(1–2):11–17

SANTI PA, JOHNSON SB, HILLENBRAND M, GRANDPRE PZ, GLASS TJ, LEGER JR (2009) Thin-sheet laser imaging microscopy for optical sectioning of thick tissues. BioTech 46(4):287–294. doi:10.2144/000113087

SATO E, SHICK HE, RANSOHOFF RM, HIROSE K (2010) Expression of fractalkine receptor CX3CR1 on cochlear macrophages influences survival of hair cells following ototoxic injury. J Assoc Res Otolaryngology : JARO 11(2):223–234. doi:10.1007/s10162-009-0198-3

SCHEIBE F, HAUPT H (1985) Biochemical differences between perilymph, cerebrospinal fluid and blood plasma in the guinea pig. Hear Res 17(1):61–66

Schnieder EA (1974) A contribution to the physiology of the perilymph. 1. The origins of perilymph. Ann Otol Rhinol Laryngol 83(1):76–83

Shi X (2010) Resident macrophages in the cochlear blood-labyrinth barrier and their renewal via migration of bone-marrow-derived cells. Cell Tissue Res 342(1):21–30. doi:10.1007/s00441-010-1040-2

Suzuki M, Kaga K (1999) Development of blood-labyrinth barrier in the semicircular canal ampulla of the rat. Hear Res 129(1–2):27–34

Suzuki M, Yamasoba T, Kaga K (1998) Development of the blood-labyrinth barrier in the rat. Hear Res 116(1–2):107–112

Tachibana M, Sankar R, Domer F (1981) Effects of acute hypertension on the extravasation of macromolecule in the temporal bone—the possible involvement of the blood-inner ear barrier. Arch Otorhinolaryngol 232(1):11–19

Takeshita Y, Ransohoff RM (2012) Inflammatory cell trafficking across the blood-brain barrier: chemokine regulation and in vitro models. Immunol Rev 248(1):228–239. doi:10.1111/j.1600-065X.2012.01127.x

Tauseef M, Knezevic N, Chava KR, Smith M, Sukriti S, Gianaris N, Obukhov AG, Vogel SM, Schraufnagel DE, Dietrich A, Birnbaumer L, Malik AB, Mehta D (2012) TLR4 activation of TRPC6-dependent calcium signaling mediates endotoxin-induced lung vascular permeability and inflammation. J Exp Med 209(11):1953–1968. doi:10.1084/jem.20111355

Thalmann I, Comegys TH, Liu SZ, Ito Z, Thalmann R (1992) Protein profiles of perilymph and endolymph of the guinea pig. Hear Res 63(1–2):37–42

Thorne M, Salt AN, DeMott JE, Henson MM, Henson OW Jr, Gewalt SL (1999) Cochlear fluid space dimensions for six species derived from reconstructions of three-dimensional magnetic resonance images. Laryngoscope 109(10):1661–1668. doi:10.1097/00005537-199910000-00021

Trune DR (1997) Cochlear immunoglobulin in the C3H/lpr mouse model for autoimmune hearing loss. Otolaryngology–Head Neck Surg : Off J Am Acad Otolaryngology-Head Neck Surg 117(5):504–508

Veszelka S, Urbanyi Z, Pazmany T, Nemeth L, Obal I, Dung NT, Abraham CS, Szabo G, Deli MA (2003) Human serum amyloid P component attenuates the bacterial lipopolysaccharide-induced increase in blood-brain barrier permeability in mice. Neurosci Lett 352(1):57–60

Wang H, Sun J, Goldstein H (2008) Human immunodeficiency virus type 1 infection increases the in vivo capacity of peripheral monocytes to cross the blood-brain barrier into the brain and the in vivo sensitivity of the blood-brain barrier to disruption by lipopolysaccharide. J Virol 82(15):7591–7600. doi:10.1128/JVI.00768-08

Wang W, Deng M, Liu X, Ai W, Tang Q, Hu J (2011) TLR4 activation induces nontolerant inflammatory response in endothelial cells. Inflammation 34(6):509–518. doi:10.1007/s10753-010-9258-4

Williams K, Alvarez X, Lackner AA (2001) Central nervous system perivascular cells are immunoregulatory cells that connect the CNS with the peripheral immune system. Glia 36(2):156–164

Wispelwey B, Lesse AJ, Hansen EJ, Scheld WM (1988) Haemophilus influenzae lipopolysaccharide-induced blood brain barrier permeability during experimental meningitis in the rat. J Clin Invest 82(4):1339–1346. doi:10.1172/JCI113736

Zhang W, Dai M, Fridberger A, Hassan A, Degagne J, Neng L, Zhang F, He W, Ren T, Trune D, Auer M, Shi X (2012) Perivascular-resident macrophage-like melanocytes in the inner ear are essential for the integrity of the intrastrial fluid-blood barrier. Proc Natl Acad Sci U S A 109(26):10388–10393. doi:10.1073/pnas.1205210109

Zhang F, Zhang J, Neng L, Shi X (2013) Characterization and inflammatory response of perivascular-resident macrophage-like melanocytes in the vestibular system. J Assoc Res Otolaryngology : JARO 14(5):635–643. doi:10.1007/s10162-013-0403-2

Zhou H, Lapointe BM, Clark SR, Zbytnuik L, Kubes P (2006) A requirement for microglial TLR4 in leukocyte recruitment into brain in response to lipopolysaccharide. J Immunol 177(11):8103–8110

Zou J, Pyykko I, Counter SA, Klason T, Bretlau P, Bjelke B (2003) In vivo observation of dynamic perilymph formation using 4.7 T MRI with gadolinium as a tracer. Acta Otolaryngol 123(8):910–915